Application of liquid dynamics theory to the glass transition

Duane C. Wallace
Theoretical Division, Los Alamos National Laboratory, Los Alamos, New Mexico 87545
(Received 29 June 1999)

In monatomic liquid dynamics theory, the system moves among a large number of intersecting nearly harmonic valleys in the many-particle potential energy surface. The same potential surface underlies the motion of atoms in the supercooled liquid. As temperature is decreased below the melting temperature, the motion among the potential valleys will begin to freeze out, and the system will pass out of equilibrium. It is therefore necessary to develop a nonequilibrium theory, based on the Hamiltonian motion. The motion is separated into two distinct parts, and idealized as follows: (a) the vibrational motion within a single valley is assumed to be purely harmonic, and remaining in equilibrium; and (b) the transit motion, which carries the system from one valley to another, is assumed to be instantaneous, and energy and momentum conserving. This idealized system is capable of exhibiting a glass transition behavior. An elementary model, incorporating the idealized motion, is the independent atom model, originally developed to treat self diffusion in monatomic liquids. For supercooled liquids, in the independent atom model, the vanishing of self diffusion at a finite temperature implies the same property for the transit probability. The vanishing of the transit probability at a finite temperature supports the view that transits are not merely thermally activated, but are controlled by phase-space correlations. For supercooled liquid sodium, the transit probability has Vogel-Tamann-Fulcher temperature dependence. The independent atom model is shown to be capable of exhibiting all the essential glass transition properties, including rate dependence of the glass transition temperature, and both exponential and nonexponential relaxation. [S1063-651X(99)01412-9]

PACS number(s): 64.70.Pf, 61.20.Gy, 66.20.+d, 61.43.Dq

I. INTRODUCTION

Liquid dynamics theory describes the motion of atoms in the liquid state. Over the years, the main problem in developing this theory has been to understand the nature of the many-particle potential energy surface upon which the liquid atoms move. Early on, Frenkel [1,2] argued that atomic motion consists mainly of vibrations about equilibrium positions, while occasionally the equilibrium positions also move. Stillinger and Weber [3–7] used the computer to find inherent structures, which are local potential minima in the many-particle potential surface. LaViolette and Stump [8] varied the interatomic potential and density, and found a variety of structural symmetries. More recently, we argued that the potential surface for a monatomic system is composed of a large number of intersecting nearly harmonic valleys, that these are divided into the classes of random and symmetric, and the random valleys dominate the statistical mechanics of the liquid state because they are vastly most numerous. On this basis we constructed a liquid dynamics Hamiltonian, evaluated the canonical partition function, and achieved agreement between theory and experiment for the thermodynamic properties of liquid metals [9,10]. In addition, from an investigation of the intervalley motion of the system, liquid dynamics theory has led to an independent atom model, which gives a respectable account of the velocity autocorrelation function and self diffusion [11].

When a liquid is cooled below its melting temperature, and when it does not crystallize, the system is called a supercooled liquid. From our current understanding of the motion of atoms in the liquid, it is apparent that the same description, indeed the same Hamiltonian, also applies to the supercooled liquid. The purpose of this work is to make that application, to model the predicted behavior, and to compare with experiment. We are interested in the supercooled liquid in general, and especially in the glass transition. The nature of materials in this regime is described in the reviews of Angell [12,13], Stillinger [14], and Ediger, Angell, and Nagel [15]. We will not consider the tunneling-state effects, which are common to glasses at lower temperatures [16,17]. Due to the current limited application of liquid dynamics theory, our theoretical work is limited to monatomic systems, with one extension to nonmolecular binary systems. Though laboratory measurements are scarce for these supercooled liquids, computer simulations are providing much useful data. From the detailed descriptions of the properties of glass forming materials [12–15], we conclude that the following characteristics must be exhibited by any meaningful theory of the glass transition.

(a) Upon cooling through the melting temperature, in the absence of crystallization, there is no discontinuity in thermodynamic or transport properties.

(b) Upon further cooling, a temperature is reached where the system falls out of thermodynamic equilibrium, and this glass transition temperature depends on the cooling rate.

(c) At temperatures above the glass transition, the shear viscosity exhibits a characteristic strong (apparently singular) temperature dependence.

(d) When the system is removed from equilibrium, above or below the glass transition temperature, it relaxes toward equilibrium, and nonexponential relaxation is commonly observed.

In Sec. II, the liquid dynamics Hamiltonian is applied to the supercooled liquid regime. It becomes apparent that the supercooled liquid will not be able to maintain equilibrium as temperature is lowered, and that a general nonequilibrium

theory is needed. Based on the Hamiltonian, the outline of this theory is developed. In Sec. III, glass transition behavior of transport properties is accounted for by the independent atom model, through the slowing down of intervalley transits as temperature is lowered. In Sec. IV, glass transition behavior of the internal energy is accounted for by the same model, after removing the degeneracy of the potential energy valleys, again through the same slowing down of intervalley transits. Our conclusions are summarized in Sec. V, our main conclusion being that the independent atom model expresses a realistic approximation to glass transition physics.

II. DYNAMICS OF THE SUPERCOOLED LIQUID

The classification of potential energy valleys as random or symmetric is an important step in clarifying the nature of the many-particle potential energy surface [9]. The symmetric valleys can be crystalline, microcrystalline, or just have some remnant of crystal symmetry among near neighbors, as in the example of amorphous carbon, where nearly all atoms have four nearest neighbors in distorted tetrahedral arrangements [18]. Because of the wide variety of possible symmetries, the symmetric valleys have a wide range of shapes, and this wide range complicates the system Hamiltonian. In contrast, the random valleys have only random near-neighbor symmetry, that is, they have no order parameter, and hence must all have the same shape (in the thermodynamic limit). Further, because of their randomness, the random valleys must be of overwhelming numerical superiority, hence they are the only valleys which need be included in the liquid dynamics Hamiltonian. We have recently concluded a molecular-dynamics study which strongly confirms these properties of the many-particle potential surface, for a potential which accurately represents metallic sodium [19,20].

The liquid dynamics classical statistical mechanics has been presented [9]. Here we present the quantum statistics, to enable the low temperature description. First consider a single random valley. The structural potential Φ_0 is the system potential at the bottom of the valley. The normal modes of oscillation around the valley bottom are labeled $\lambda = 1,...,3N$ for an N-particle system, and normal mode λ has momentum p_λ, displacement q_λ, and frequency ω_λ. Then the quasiharmonic Hamiltonian for the system within this random valley is

$$H_H = \Phi_0 + \sum_\lambda \left[\frac{p_\lambda^2}{2M} + \frac{1}{2} M \omega_\lambda^2 q_\lambda^2 \right], \tag{1}$$

where M is the atomic mass. The complete liquid dynamics Hamiltonian is the sum of quasiharmonic Hamiltonians (1) over all random valleys in the potential surface, plus corrections for the anharmonicity of each valley, plus corrections for the boundary where valleys intersect. To evaluate the partition function, two observations are important. First, the parameters Φ_0 and $\{\omega_\lambda\}$ are the same for every random valley, so we merely have to evaluate the quasiharmonic partition function for one valley, and multiply by w^N, the total number of random valleys. From a careful analysis of the entropy of melting for normal-melting elements, we have found the universal value $\ln w = 0.8$ [9,21]. Second, the anharmonic and boundary contributions are small, and can be treated in perturbation theory. When the algebra is done, the Helmholtz free energy becomes [22]

$$F = \Phi_0 - NkT \ln w + \sum_\lambda \left[\frac{1}{2} \hbar \omega_\lambda - kT \ln(n_\lambda + 1) \right] + F_A + F_B, \tag{2}$$

where F_A and F_B respectively express the anharmonic and boundary contributions. The corresponding internal energy U, and entropy S are given by

$$U = \Phi_0 + \sum_\lambda \hbar \omega_\lambda \left(n_\lambda + \frac{1}{2} \right) + U_A + U_B, \tag{3}$$

$$S = Nk \ln w + k \sum_\lambda \left[(n_\lambda + 1) \ln(n_\lambda + 1) - n_\lambda \ln n_\lambda \right] + S_A + S_B, \tag{4}$$

where n_λ is the boson occupation number,

$$n_\lambda = \frac{1}{e^{\hbar \omega_\lambda / kT} - 1}. \tag{5}$$

Finally, since in this paper we are only interested in properties depending on the motion of the atoms, the electronic-excitation contributions are neglected throughout (see, e.g., Refs. [9] and [22]).

We are now ready to identify the limits of equilibrium statistical mechanics for the problem at hand. First note, the partition function we have constructed is *approximate*, because the system phase space has been limited to just the random valleys in the many-particle potential surface. But this limited phase space should be a good approximation, not only for the liquid, but also for the supercooled liquid, even though the supercooled liquid is metastable. Accordingly, the supercooled liquid equilibrium thermodynamic functions are given by Eqs. (2)–(5). Now a problem arises. The entropy [Eq. (4)] contains the constant term $Nk \ln w$, expressing that the system visits the entire collection of random valleys. But in reality, when the system is cooled from the liquid, at some temperature its motion among the random valleys begins to freeze out, and then the valleys are no longer equally accessible, and the entropy is not defined. To treat the system in this regime, we have to abandon equilibrium statistical mechanics, at least for the nonequilibrium degrees of freedom, and return to the Hamiltonian-induced motion of the system, as it moves among nonequilibrium states.

To proceed with this program, let us consider the system in any state, and separate the motion into two distinct parts: the motion within a single random valley, called the vibrational motion, and the motion from one valley to another, called a transit. To simplify the picture, we will idealize each type of motion, keeping only its essential physical character.

In the vibrational motion, we keep only the quasiharmonic part, and assume that the vibrational interactions (the anharmonicity) are sufficient to maintain this quasiharmonic part in internal thermodynamic equilibrium. Under this condition, a temperature is defined, the vibrational free energy remains physically meaningful, and can be written

$$F_{\rm vib}=\Phi_0+\sum_\lambda\left[\frac{1}{2}\hbar\omega_\lambda-kT\ln(n_\lambda+1)\right]. \tag{6}$$

We have previously observed that transits are local, i.e., each transit corresponds to a change in the equilibrium positions of only a small group of neighboring atoms [9,11]. For the present let us assume that each transit is instantaneous in time, and conserves total energy and momentum among the transiting atoms. Then the transits make no contribution to the system energy, and their sole function is to move the system among the many available potential energy valleys. This idealization provides for a simple resolution of the system properties, as follows.

(a) Since the energy is all vibrational, the total energy is just the quasiharmonic contribution from Eq. (6),

$$U=U_{\rm vib}=\Phi_0+\sum_\lambda\hbar\omega_\lambda\left(n_\lambda+\frac{1}{2}\right). \tag{7}$$

The system temperature is defined through the equilibrium distribution n_λ, given by Eq. (5).

(b) While the transit rate is extremely high in the equilibrium liquid, it should decrease strongly as temperature is lowered below melting. It is this slowing down which expresses the freezing out of the intervalley motion.

(c) There is no discontinuity in thermodynamic or transport properties at the melting temperature.

(d) Along with the slowing of the transit rate, as temperature is lowered for the supercooled liquid, self diffusion will decrease, and viscosity will increase, similar to the behavior of real liquids as the glass transition is approached. We have previously developed an independent atom model to describe self diffusion in the monatomic liquid state, and in Sec. III we will apply this model to the supercooled liquid, and will extract the underlying relation between glass transition behavior and the slowing of the transit rate.

(e) Though transport properties are sensitive to the transit rate, as just mentioned, the internal energy (7) is independent of the transit rate. This is because every random valley has the same potential parameters Φ_0 and $\{\omega_\lambda\}$. Hence for a monatomic system constrained to move only among random valleys, the system energy will not show evidence of a glass transition. However, for a more complicated system, like for example a binary system composed of A and B atoms, the structural potential Φ_0 will depend on the A-A, B-B, and A-B correlations, so that Φ_0 will split into a band of energies. Now the system can relax among valleys of unequal potential energy, and as the transit rate slows with decreasing temperature, the internal energy will exhibit a glass transition. An independent atom model capturing this effect will be studied in Sec. IV.

III. INDEPENDENT ATOM MODEL FOR THE TRANSPORT GLASS TRANSITION

The experimental quantity which perhaps most universally typifies the glass transition is the shear viscosity η. Angell [12] showed that the temperature dependence of η for all glass forming liquids is qualitatively rationalized by the single Vogel-Tamann-Fulcher (VTF) function,

$$\eta=A\exp\left(\frac{BT_0}{T-T_0}\right), \tag{8}$$

where A, B, and T_0 are positive parameters. The variation in shape of the $\eta(T)$ curves, from fragile to strong glass formers, is reproduced by the variation of B from small to large, respectively [12]. The important point for our discussion is that the temperature dependence of viscosity is much stronger than Arrhenius, and indeed the use of Eq. (8) to fit $\eta(T)$ data indicates that $\eta\to\infty$ at the finite temperature T_0.

While we have not completed application of liquid dynamics theory to shear viscosity, we have treated self diffusion in the liquid state [11], and have done extensive molecular-dynamics (MD) calculations of the self diffusion coefficient D for supercooled liquid sodium [19]. The following evidence indicates that the essential glass transition behavior of $\eta(T)$ is also present in $D(T)$. First, consider the Stokes-Einstein relation

$$D=\frac{kT}{b\eta}, \tag{9}$$

where b is a distance on the atomic scale. When Eq. (9) is used to relate experimental data for D and η, b is found to be nearly temperature independent for a given liquid (data for Lennard-Jones argon at liquid density are given in Ref. [23], and data for liquid sodium are given in refs. [24–26]). Second, the common result of MD calculations is that, within limits of computational error, D appears to go to zero at a finite temperature (see Refs. [27] and [28], and especially Fig. 10 of Ref. [19]). We will therefore consider the temperature dependence of D as an appropriate expression of glass transition behavior.

In applying liquid dynamics theory to self diffusion in a monatomic liquid, the following argument led us to develop the independent atom model. First, to calculate the partition function, the normal vibrational modes for each many-particle valley are quite useful, as is demonstrated by results (2)–(5) for the equilibrium thermodynamic functions. However, to follow the actual motion of the atoms, the normal modes lose their utility, because the very high rate of transits causes the normal mode eigenvectors for any single atom to change many times during one mean vibrational period of the atom. Hence each atom ''sees'' a rapidly fluctuating potential well, due to its neighbors, and the leading approximation to this fluctuating well is its time average, which is a constant nearly harmonic well, the same for every atom. The independent atom model allows each atom to move classically through a set of identical harmonic wells, and at each turning point the atom may move forward into a new well, or may move back in the same well. An algebraic expression is obtained for the velocity autocorrelation function, and the self diffusion coefficient is found to be [11]

$$D=\frac{4kT}{\pi M\omega}\left(\frac{\xi}{2-\xi}\right), \tag{10}$$

where M is the atomic mass, ω is the vibrational frequency of each isotropic three-dimensional well, and ξ is a parameter discussed below. The independent atom model gives encouraging agreement with the velocity autocorrelation function

for liquid alkali metals, and with experimental values of D for liquid metals, where ω is always close to the mean vibrational frequency in the liquid [11].

According to Eq. (10), if D vanishes at finite T, then ξ must have the same property. The parameter is given by [11]

$$\xi=[1-\langle\cos\theta\rangle]\mu, \tag{11}$$

where μ is the probability that an atom will transit when it reaches a turning point, with $0\leqslant\mu\leqslant 1$, and $\langle\cos\theta\rangle$ is the average change in the atom's displacement direction-cosine at the transit. But $\langle\cos\theta\rangle$ can have little temperature dependence [11], and we can set $\xi\approx\frac{3}{2}\mu$ as an approximation, so the important temperature dependence of ξ resides in the transit probability μ. We have already expressed the idea that transits are controlled, not by *thermal activation*, but by correlations [11]. Suppose for example that a small group of two or three atoms is prepared to make a transit. The transit will occur only if these atoms, plus a number of their neighbors, are all in the right place at the right time, so that each transiting atom sees a clear path to move on to a new equilibrium position. More precisely, each transit occupies only a small volume, call it a window, in the many-particle phase space. In the liquid state, the transit probability is large, say at $\mu\gtrsim\frac{1}{2}$, which means the system easily finds the transit windows. Further, since μ is bounded by 1, then μ can increase only weakly as T increases above T_m, and this property is in agreement with all available velocity autocorrelation and self diffusion data for liquid metals [11]. On the other hand, as T decreases below T_m, the many-particle phase space sampled by the system decreases strongly, until the system is virtually unable to find a transit window. We therefore expect μ to become essentially zero at a finite temperature.

Let us use our MD calculations for supercooled liquid sodium [19], to test the above picture. The characteristic temperature for random valleys is $\theta_2=154.0$ K, and this gives $\omega_2=1.562\,(10^{13}/\mathrm{s})$ for the rms normal mode frequency [Eqs. (3.6) and (3.7) of Ref. [19]]. With $\omega=\omega_2$, we used Eq. (10) to find ξ from each of our calculated values of D, and the results are graphed in Fig. 1. The $\xi(T)$ data are fitted quite well by the VTF function with only one adjustable parameter

$$\xi(T)=\exp\left(\frac{-T_0}{T-T_0}\right), \tag{12}$$

with $T_0=121$ K. Hence $\xi(T)$ for supercooled liquid sodium has stronger-than-Arrhenius temperature dependence, and appears to go to zero at around 121 K. For comparison, sodium melts at 371 K. We draw three conclusions from the above results.

(a) In supercooled liquid dynamics, the transport glass transition results from a strong decrease of the transit rate with decreasing temperature. In the independent atom model, this appears as a VTF temperature dependence of $\xi(T)$, and hence also of $\mu(T)$.

(b) The strong temperature dependence of μ, and especially the vanishing of μ at a finite temperature, is consistent with the view that transits are controlled by phase-space correlations.

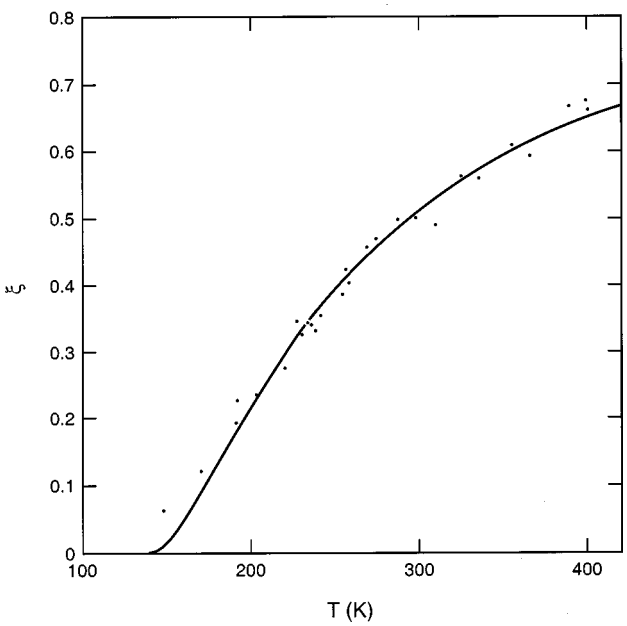

FIG. 1. Points are values of ξ extracted from MD calculations of D for supercooled liquid sodium, and the line is the fitted VTF function with $T_0=121$ K. Each ξ is within its estimated error of the line, except for the point at 310 K.

(c) Since our analysis has so far been limited to $T>T_m$ for the velocity autocorrelation function [11], and has been limited in Fig. 1 to $\xi\gtrsim 0.1$, additional calculations of these quantities at lower temperatures would further clarify the nature of the transport glass transition.

IV. INDEPENDENT ATOM MODEL FOR THE THERMAL GLASS TRANSITION

Let us now extend the independent atom model, to endow it with a thermal glass transition. To do this, according to the discussion in Sec. II, it is necessary to remove the energy degeneracy of the independent atom potential wells. We will construct the simplest possible model. The independent atom is allowed to oscillate in either of two isotropic three-dimensional harmonic wells, and to transit between the wells, with some probability, at each turning point. The potential minimum of well 2 is at zero, the potential minimum of well 1 is at $\Delta>0$, and each well has frequency ω. The atom has total energy E, so that its mean kinetic energy in well 2 is $\mathcal{K}_2=\frac{1}{2}E$, and its mean kinetic energy in well 1 is $\mathcal{K}_1=\frac{1}{2}(E-\Delta)$. Our system consists of N such atoms, each with energy E, with N_1 in well 1 and N_2 in well 2, where $N_1+N_2=N$. The mean kinetic energy of the entire system is $N\mathcal{K}$, where $\mathcal{K}$ is given by

$$\mathcal{K}=n_1\mathcal{K}_1+n_2\mathcal{K}_2, \tag{13}$$

and $n_1=N_1/N$, $n_2=N_2/N$. We assume there are interactions among the oscillating atoms, and these interactions keep the system kinetic energy in an equilibrium distribution. This distribution is characterized by the temperature T, and we neglect quantum effects for simplicity, and take the classical relation $\mathcal{K}=\frac{3}{2}kT$. The information in the above equations is then expressed in the form

$$E=3kT+n_1\Delta. \tag{14}$$

Since no energy is to be associated with the transits, E is the thermodynamic internal energy per atom, or $NE=U$.

At a turning point, an atom in well 1 has probability μ_1 of transiting to well 2, and an atom in well 2 has probability μ_2 of transiting to well 1. Since the time between turning points is π/ω, the rate per atom of transiting out of well 1 is $R_1=(\pi/\omega)\mu_1$, and the rate per atom of transiting out of well 2 is $R_2=(\pi/\omega)\mu_2$. Then the time rates of change of the occupation numbers n_1 and n_2 are given by

$$\begin{aligned}\dot{n}_1&=-n_1R_1+n_2R_2,\\ \dot{n}_2&=n_1R_1-n_2R_2,\end{aligned} \tag{15}$$

or, eliminating n_2,

$$\dot{n}_1=R_2-n_1(R_1+R_2). \tag{16}$$

Following the results of Sec. III, we model μ_1 and μ_2 with VTF functions, each containing a single parameter in the form of a critical temperature, so that

$$\begin{aligned}R_1&=\frac{\pi}{\omega}\exp\left(\frac{-T_1}{T-T_1}\right)\quad \text{for } T\geqslant T_1,\\ R_1&=0\quad \text{for } T\leqslant T_1,\\ R_2&=\frac{\pi}{\omega}\exp\left(\frac{-T_2}{T-T_2}\right)\quad \text{for } T\geqslant T_2,\\ R_2&=0\quad \text{for } T\leqslant T_2.\end{aligned} \tag{17}$$

Since well 1 lies at potential above well 2, we expect $T_1<T_2$. But T_1 should be near T_2, so that R_1 and R_2 slow down together, to achieve glass transition behavior.

The complete evolution of the system is given by Eq. (14) for the internal energy, and Eq. (16) for the relaxation of n_1. The independent variables are T and n_1, and the model contains the four parameters T_1, T_2, Δ, and ω. We will scale temperature with T_2, and will scale time with the vibrational period $\tau=2\pi/\omega$, so that the characteristic properties of the model can be expressed in terms of the two parameters T_1/T_2 and Δ.

Our first calculation is of the equilibrium curve for $n_1(T)$. The equilibrium condition is $\dot{n}_1=0$, and from Eq. (16) this gives

$$n_1(\text{eq})=\frac{R_2}{R_1+R_2}. \tag{18}$$

This tells us that $n_1(\text{eq})\to\frac{1}{2}$ as $T\to\infty$, and $n_1(\text{eq})\to 0$ as T decreases to T_2. Between these limits, the shape of the curve depends on T_1/T_2, as shown in Fig. 2. Hence the independent atom model possesses a one-parameter family of equilibrium curves. On each equilibrium curve, according to Eq. (14), the internal energy per atom is the thermal contribution $3kT$, plus the potential term $n_1\Delta$, with n_1 shown in Fig. 2.

Let us next calculate $n_1(T)$ under the condition that our system is placed in equilibrium at a high temperature, and is then cooled at the constant rate γ, defined by

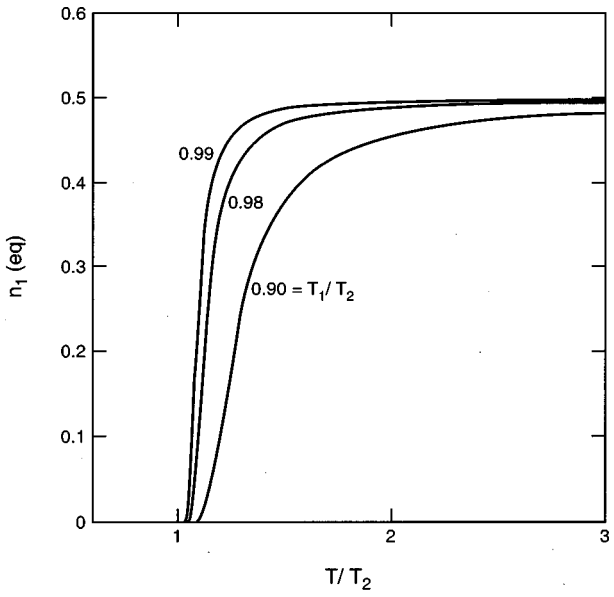

FIG. 2. The equilibrium curves $n_1(\text{eq})$ vs T/T_2, for various T_1/T_2 values.

$$\dot{T}/T_2=-\gamma. \tag{19}$$

$n_1(T)$ is obtained by simultaneous integration of Eq. (19) for $\dot{T}$, and Eq. (16) for $\dot{n}_1$. In the process, the system remains near equilibrium, and $n_1(T)$ follows just above the equilibrium curve, down to some temperature, and then the system passes out of equilibrium and freezes into a state with nonzero n_1. Representative curves are shown in Fig. 3, for $T_1/T_2=0.98$, and for a range of cooling rates as expressed by the dimensionless variable $\gamma\tau$. If the temperature at which the system passes out of equilibrium is the glass transition temperature T_g, then clearly our system exhibits a rate-dependent T_g. The curves in Fig. 3 are similar to the curves

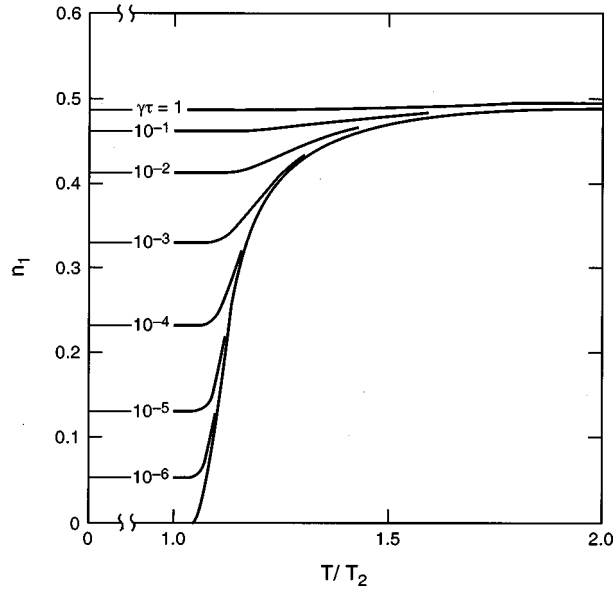

FIG. 3. Curves of n_1 vs T/T_2 for cooling from equilibrium at the constant rates labeled by values of $\gamma\tau$. T_1/T_2 is 0.98, and the lower envelope curve is n_1 (eq).

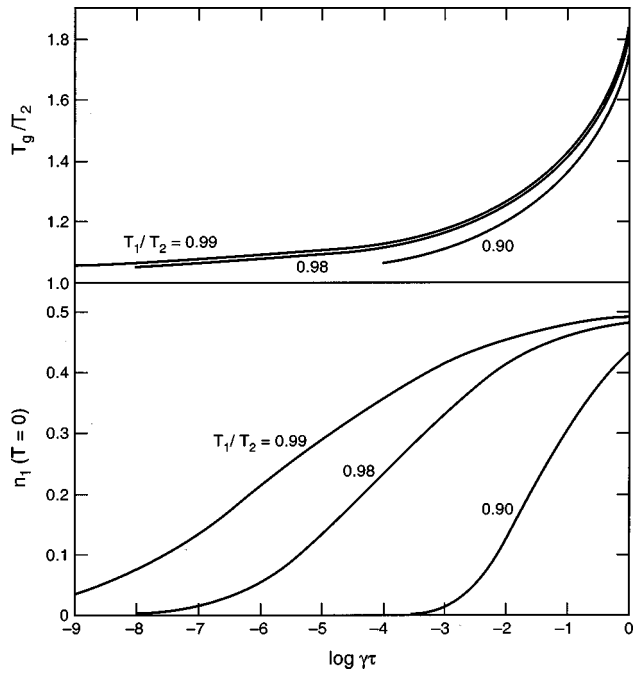

FIG. 4. The glass transition temperature T_g/T_2 is shown in the upper panel as a function of cooling rate $\gamma\tau$ and for several values of T_1/T_2, and n_1 frozen in at zero temperature is shown in the lower panel. The log function is base 10.

sketched by Ediger, Angell, and Nagel (Fig. 1 of Ref. [15]), to illustrate rate dependence of T_g. In addition, the curves of Fig. 3 exhibit a property described by Angell, Clarke, and Woodcock [29], in their discussion of computer experiments on glass formation, namely, that the glass transition becomes sharper as the cooling rate is lowered.

For a given cooling rate, let us define T_g as the temperature at which $n_1(\mathrm{eq})$ is equal to the zero-temperature frozen-in value of n_1 (see Fig. 3). With this definition, T_g is always above T_2. Our results are shown in Fig. 4, where it is seen that T_g decreases monotonically with the cooling rate, and the curve depends on T_1/T_2. The zero-temperature frozen-in value of n_1 varies from $\frac{1}{2}$ at infinite cooling rate, to zero at zero cooling rate, and the crossover cooling rate is strongly dependent on T_1/T_2. Again our results are shown in Fig. 4. In an experiment on a real material, one might not be able to measure n_1 directly, but would presumably be able to measure the frozen-in potential energy $n_1\Delta$ per atom [see Eq. (14)]. The shapes of the curves in Fig. 4, for T_g and $n_1(T=0)$ vs the cooling rate, are similar to those obtained by Vollmayr, Kob, and Binder [30], from large scale computer simulations of binary Lennard-Jones systems (their Figs. 5 and 6, respectively).

The final property we wish to discuss is relaxation toward equilibrium. Suppose our system is removed from equilibrium, to any point on the graph of Fig. 2, and is then allowed to relax. There are three relaxation regions:

$$T<T_1;\quad R_1=R_2=0,$$

$$T_1<T<T_2;\quad R_1>0, R_2=0, \tag{20}$$

$$T_2<T;\quad R_1>0, R_2>0.$$

For $T<T_1$, no relaxation occurs, and for $T_1<T<T_2$, the relaxation is *extremely* slow for the model parameters we are studying. To keep the discussion simple, let us consider $T_2<T$, which still allows for T above or below T_g. We will examine relaxation for isothermal and adiabatic processes.

In isothermal relaxation, the temperature is held constant, so the rates R_1 and R_2, given by Eq. (17), are each constant. The relaxation equation (16) can be written for $\delta n_1 = n_1 - n_1(\mathrm{eq})$, as

$$\delta\dot{n}_1 = -\delta n_1(R_1+R_2). \tag{21}$$

Hence the relaxation is exponential, with relaxation time $(R_1+R_2)^{-1}$.

In adiabatic relaxation, the system is thermally isolated, so its energy E is constant. From Eq. (14), the condition $\dot{E}=0$ is

$$3k\dot{T} = -\Delta\dot{n}_1. \tag{22}$$

The relaxation is calculated by simultaneous integration of Eqs. (16) and (22). The process is sensitive to the magnitude of Δ in Eq. (22). The system relaxes to a point on the equilibrium curve, so the functions $\delta n_1 = n_1 - n_1(\mathrm{eq})$, and $\delta T = T - T(\mathrm{eq})$, relax to zero. The constant energy constraint is $\delta E(t)=0$ for all t, and setting $\delta E(t)=\delta E(0)$, Eq. (14) yields

$$\frac{\delta T(t)}{\delta T(0)} = \frac{\delta n_1(t)}{\delta n_1(0)}. \tag{23}$$

Hence there is only one independent relaxation function. Results of our calculations are as follows.

(a) If the initial state lies above the equilibrium curve in Fig. 2, then n_1 decreases toward equilibrium, and correspondingly T increases [Eq. (22)]. As T increases, the rates R_1 and R_2 increase, causing the relaxation to proceed faster than exponentially in time.

(b) If the initial state lies below the equilibrium curve in Fig. 2, then n_1 increases toward equilibrium, and correspondingly T decreases [Eq. (22)]. As T decreases, the rates R_1 and R_2 decrease, causing the relaxation to proceed slower than exponentially in time.

(c) In the limit as the system come near the equilibrium curve of Fig. 2, from above or below, the relaxation approaches exponential in time.

V. SUMMARY OF CONCLUSIONS

Supercooled liquid dynamics

In monatomic liquid dynamics theory, the system moves among a large number of intersecting nearly harmonic random valleys in the many-particle potential surface. The same potential surface underlies the motion of atoms in the supercooled liquid. The quantum thermodynamic functions are given by Eqs. (2)–(5), and contain the entropy constant $Nk\ln w$, expressing motion of the system among all the random valleys. In reality, however, as temperature is lowered below T_m, at some temperature the motion among random valleys will begin to freeze out, and then the entropy is no longer defined. We therefore have to develop a nonequilib-

rium theory, based on the Hamiltonian motion of the system. The motion is separated into two parts, and each part is idealized to its essential physical character. The following description emerges.

The vibrational motion is the motion of the system in any single random potential valley. This is assumed to be purely harmonic, with anharmonicity serving to keep the vibrational motion in equilibrium. The system energy is entirely vibrational, so the internal energy is the vibrational energy, [Eq. (7)], and temperature is defined through the equilibrium distribution n_λ [Eq. (5)].

A transit is the motion of the system in passing from one valley to another. Transits are assumed to be instantaneous, and energy and momentum conserving, so that their sole function is to move the system among the available valleys.

There is no discontinuity in thermodynamic or transport properties as the system is cooled through T_m. However, as temperature is decreased below T_m, the transit rate decreases, giving rise to a glass transition in the transport properties. Because all random valleys have the same potential parameters, for a monatomic system, the internal energy will not show evidence of a glass transition. However for a binary system, for example, the random valleys will acquire a range of potential parameters, and now the slowing of the transit rate gives rise to a glass transition in the internal energy.

Transport glass transition

We want an elementary model incorporating the above physical properties, and for which we can calculate the nonequilibrium evolution under any condition. The independent atom model, originally developed to treat self diffusion in the liquid, serves this purpose. An atom moves through a set of identical isotropic three-dimensional harmonic wells, each with frequency ω, and at each turning point the atom moves forward into a new well with probability μ, or moves back in its old well with probability $1-\mu$. The system is a collection of such atoms, with the appropriate physical variables, such as amplitudes and phases, being averaged over the collection. The independent atom model has been justified as a leading approximation to the atomic motion, by averaging out the fluctuations in the potential field ''seen'' by a single atom in the liquid state [11].

The independent atom model gives Eq. (10) for the self diffusion coefficient D, where $\xi \approx \mu$. To apply the independent atom model to the supercooled liquid, we used our computer calculations for metallic sodium to find $\xi(T)$ at $T \lesssim T_m$. The result is shown in Fig. 1, and leads to the following conclusions.

$\xi(T)$ is well fitted by the VTF function with $T_0 = 121\,\mathrm{K}$. The same temperature dependence applies to the transit probability $\mu(T)$, supporting the view that transits are not merely thermally activated, but are limited by correlations among the atoms involved in a transit. Thus a transit has only a small window in the many-particle phase space, and the phase space sampled by the system decreases strongly as temperature decreases, causing μ to become essentially zero at a finite temperature.

Directly as a result of the slowing down of the transit rate with decreasing temperature, the self diffusion and viscosity exhibit glass transition behavior. To further clarify the glass transition process, additional calculations are needed of the velocity autocorrelation function at $T \lesssim T_m$, and of ξ or μ at values $\lesssim 0.1$.

Thermal glass transition

To obtain a thermal glass transition in the independent atom model, the atom is allowed to move within two wells, each with frequency ω, but with well 1 lying higher than well 2. The transit probabilities μ_1 out of well 1, and μ_2 out of well 2, are modeled with VTF functions having critical temperatures T_1 and T_2, respectively, with $T_1 < T_2$. The ratio T_1/T_2 becomes an important parameter of the model. Our calculations lead to the following conclusions.

In equilibrium, the occupation numbers are $n_1 = n_2 = \frac{1}{2}$ at $T = \infty$, and well 1 gradually empties as T decreases, until $n_1 = 0$ at $T = T_2$. The shape of the intervening equilibrium curve depends on T_1/T_2 (Fig. 2).

Upon cooling at a constant rate, from an equilibrium state at high temperature, the system remains near equilibrium down to the glass transition temperature T_g, then the system passes out of equilibrium and freezes into a state with nonzero n_1. T_g decreases, and the glass transition becomes sharper, as cooling rate decreases (Fig. 3). Curves of T_g vs cooling rate, and of the frozen-in value of n_1 vs cooling rate, depend on T_1/T_2 (Fig. 4). The shapes of these curves are similar to results of large-scale computer simulations [30].

When the system is removed from equilibrium and allowed to relax isothermally, the relaxation is exponential in time. When the system is allowed to relax adiabatically, the relaxation is nonexponential in general, but approaches exponential as the system comes arbitrarily close to equilibrium.

In our view, though the independent atom model is a severe idealization of real systems, expressing the motion as a combination of vibrations and transits captures the underlying nature of real glass transition behavior. In a simple and natural manner, the independent atom model accounts for the four main characteristics of the glass transition, as listed in Sec. I, plus further details actually found in large-scale computer simulations.

ACKNOWLEDGMENTS

We are grateful for the collaboration of Bradford Clements, who has strongly influenced this research. The work was supported in part by the Department of Energy under Contract No. W-7405-ENG-36

[1] J. Frenkel, Z. Phys. **35**, 652 (1926).
[2] J. Frenkel, *Kinetic Theory of Liquids* (Clarendon, Oxford, 1946), Chap. III, Sec. 1.
[3] F. H. Stillinger and T. A. Weber, Kinam **3**, 159 (1981).
[4] F. H. Stillinger and T. A. Weber, Phys. Rev. A **25**, 978 (1982).
[5] F. H. Stillinger and T. A. Weber, Phys. Rev. A **28**, 2408 (1983).
[6] F. H. Stillinger and T. A. Weber, Science **225**, 983 (1984).

[7] T. A. Weber and F. H. Stillinger, J. Chem. Phys. **80**, 2742 (1984).
[8] R. A. LaViolette and D. M. Stump, Phys. Rev. B **50**, 5988 (1994).
[9] D. C. Wallace, Phys. Rev. E **56**, 4179 (1997).
[10] D. C. Wallace, Phys. Rev. E **57**, 1717 (1998).
[11] D. C. Wallace, Phys. Rev. E **58**, 538 (1998).
[12] C. A. Angell, J. Non-Cryst. Solids **102**, 205 (1988).
[13] C. A. Angell, Science **267**, 1924 (1995).
[14] F. H. Stillinger, Science **267**, 1935 (1995).
[15] M. D. Ediger, C. A. Angell, and S. R. Nagel, J. Phys. Chem. **100**, 13 200 (1996).
[16] W. A. Phillips, J. Low Temp. Phys. **7**, 351 (1972).
[17] P. W. Anderson, B. I. Halperin, and C. M. Varma, Philos. Mag. **25**, 1 (1972).
[18] D. R. McKenzie, D. Muller, and B. A. Pailthorpe, Phys. Rev. Lett. **67**, 773 (1991).
[19] D. C. Wallace and B. E. Clements, Phys. Rev. E **59**, 2942 (1999).
[20] B. E. Clements and D. C. Wallace, Phys. Rev. E **59**, 2955 (1999).
[21] D. C. Wallace, Phys. Rev. E **56**, 1981 (1997).
[22] Quantum statistical mechanics of quasiharmonic vibrational systems, with interactions, is presented in detail in D. C. Wallace, *Thermodynamics of Crystals* (Dover, New York, 1998).
[23] P. Borgelt, C. Hoheisel, and G. Stell, Phys. Rev. A **42**, 789 (1990).
[24] C. T. Ewing, J. A. Grand, and R. R. Miller, J. Am. Chem. Soc. **73**, 1168 (1951).
[25] C. T. Ewing, J. A. Grand, and R. R. Miller, J. Phys. Chem. **58**, 1086 (1954).
[26] S. J. Larsson, C. Roxbergh, and A. Lodding, Phys. Chem. Liq. **3**, 137 (1972).
[27] J. H. R. Clarke, J. Chem. Soc. Faraday Trans. 2 **75**, 1371 (1979).
[28] R. D. Mountain, Phys. Rev. A **26**, 2859 (1982); **27**, 2767 (1983).
[29] C. A. Angell, J. H. R. Clarke, and L. V. Woodcock, in *Advances in Chemical Physics*, edited by I. Prigogine and S. A. Rice (Wiley Interscience, New York, 1981), Vol. 48, p. 397.
[30] K. Vollmayr, W. Kob, and K. Binder, J. Chem. Phys. **105**, 4714 (1996).